2011 American Control Conference
on O'Farrell Street, San Francisco, CA, USA
June 29 - July 01, 2011

Adaptive Interconnected Observer for Induction Machine in Presence of Nonlinear Magnetic Characteristic

A. El Fadili, F. Giri, A. El Magri, L. Dugard, M. Haloua.

Abstract- **The problem of state estimation in induction motors is considered. Generally, the motor observer design is dealt with, based on standard models ignoring the saturation effect of the magnetic characteristic. As a matter of fact, magnetic saturation cannot be ignored especially when considering (speed, torque) control strategies that involve large flux variations. Such large variations are necessary to meet optimal operation conditions in presence of wide range load torque changes. On the other hand, it is well known that the use of mechanical (speed, torque) sensors leads to reliability issues. In this paper, a new adaptive observer design is developed for induction machine, based on a model that accounts for the nonlinear feature of the magnetic circuit. The observer provides estimates of the mechanical and magnetic variables using only stator currents and voltages measurements. The observer convergence is formally analyzed and illustrated by simulation.**

I. INTRODUCTION

WHEN controlling induction machines, measurements of electromagnetic and mechanical variables (voltages, currents, flux, speed, position, etc) are required. For some variables (e.g. stator voltages and currents), there exist reliable and not too expensive sensors providing sufficiently accurate measures. This is not the case for other variables such as the rotor flux. Then, observers should be designed, based on the machine model, to get on-line estimates of the variables which are not accessible to measurement. The first observers (see e.g. [8]) were developed based on simplified assumptions e.g., linear magnetic characteristics, constant (or slowly varying) rotor speed. Under these assumptions, the model of the induction motor becomes linear and, therefore, observability analysis and observer design may be dealt with, using standard linear theory tools (pole placement design, Luenberger and Kalman observers). Interesting contributions came out later when nonlinear observers not supposing a constant rotor speed were proposed (see e.g. [2], [4], [11]). These have been designed using different approaches such as high gain, sliding mode and dynamic state feedback. However, even in these contributions, the characteristics of the machine magnetic circuit were still supposed to be linear. As a matter of fact, this assumption is only valid when the machine operates with a flux value close to the nominal flux. But, a constant-flux operation-mode cannot be optimal when large speed variations are needed, [3]. To achieve high observation performances, regardless the machine operation mode, the observer design should be based on a model that accounts for the nonlinear feature of the machine magnetic circuit. This was done in few previous works, see e.g. [6] and [10], where the proposed observers were designed under the assumption that the mechanical speed and the load torque were measured. Due to cost reduction, mechanical speed sensor fragility, and sensor installation difficulty, sensorless induction machine drives are becoming wide spread solution for the next generation of commercial drives.

In this paper, one seeks accurate estimation of the induction machine magnetic and mechanical variables, supposing the stator current and voltage to be the only available measurements. To this end, an adaptive interconnected observer will be designed using the 'interconnected extended-Kalman filter' approach and a model that accounts for the nonlinear feature of the machine magnetic characteristic [9]. The adaptive observer thus obtained will prove to be exponentially convergent in presence of wide range flux variations, despite machine parameters uncertainty. The paper is organized as follows: induction motor modeling is dealt with in Section 2; the observer design and stability analysis are developed in Section 3; the theoretical observer performances are confirmed by numerical simulations in Section 4.

II. INDUCTION MOTOR MODELLING

In [9], a model was proposed and experimentally validated for an induction machine of 7.5 kW. The originality of the obtained model lies in the fact that it takes into account the saturation effect of the machine magnetic characteristics (fig 1). It is defined by the following state space representation:

$$J\dot{\Omega} = -f\ \Omega + p(\phi_{r\alpha} i_{s\beta} - \phi_{r\beta} i_{s\alpha}) - T_L \tag{1}$$

$$\dot{i}_{s\alpha} = -a_2 i_{s\alpha} + \delta\,\phi_{r\alpha} + a_3 p\Omega\phi_{r\beta} + a_3 u_{s\alpha} \tag{2}$$

$$\dot{i}_{s\beta} = -a_2 i_{s\beta} - a_3 p\Omega\phi_{r\alpha} + \delta\,\phi_{r\beta} + a_3 u_{s\beta} \tag{3}$$

$$\dot{\phi}_{r\alpha} = a_1 i_{s\alpha} - L_{seq}\delta\,\phi_{r\alpha} - p\Omega\phi_{r\beta} \tag{4}$$

$$\dot{\phi}_{r\beta} = a_1 i_{s\beta} - L_{seq}\delta\,\phi_{r\beta} + p\Omega\phi_{r\alpha} \tag{5}$$

δ is a varying parameter that depends on the machine magnetic state (see Fig 2). In [9], this dependence was given a polynomial approximation:

$$\delta = \mathrm{T}(\Phi_r) \tag{7}$$

$$T(\Phi_r) = q_0 + q_1\Phi_r + \ldots + q_m\Phi_r^m \tag{8}$$

where Φ_r is the amplitude of the (instantaneous) rotor flux, denoted ϕ_r. Consequently:

Manuscript received September 2, 2010.
F. Giri is with GREYC Lab, UMR CNRS, University of Caen, France.
L. Dugard is with GIPSA Lab, UMR CNRS, Grenoble-INP, France.
A. El Fadili, A. El Magri, M. Haloua are with EMI, LAII, Rabat, Morocco. Corresponding author: elfadili_abderrahim@ yahoo.fr

$$\Phi_r = \sqrt{\phi_{r\alpha}^2 + \phi_{r\beta}^2} \tag{9}$$

where $\phi_{r\alpha}, \phi_{r\beta}$ are the rotor flux $\alpha\beta$-components. The coefficients in (8) have been experimentally identified in [9] using Fig 1. The other notations in (1)-(5) are defined as follows:

$(i_{s\alpha}, i_{s\beta})$ represent the αβ-components of the stator current; Ω denotes the motor speed; R_s, R_r designate the stator and rotor resistances; T_L represents the load torque, J is the inertia of the set 'rotor-load'; p is the number of pole pairs; L_{seq} is the equivalent inductance seen by the stator of both stator and rotor leakage;

$$a_1 = R_r\,,\ a_3 = (L_{seq})^{-1}\,,\ a_2 = a_3(R_s + R_r) \tag{10}$$

The numerical values of the model parameters are described by Table 1. They have been experimentally determined in [9] for an induction motor of 7.5 KW power.

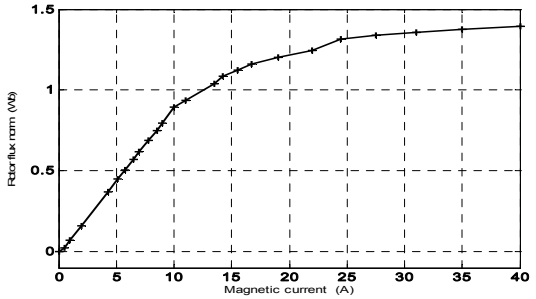

Fig 1. Magnetic characteristic experimentally obtained for a 7.5KW induction motor [9] ; rotor flux norm Φ_r (Wb) in function of the magnetic current I_μ (A).

III. INTERCONNECTED OBSERVER DESIGN

Assume that the load torque and stator resistance are slowly varying. Then, the dynamic of these two variables may approximately read as:

$$\dot{T}_l = 0, \quad \dot{R}_s = 0. \tag{11}$$

The full induction machine model (1)-(9) may be seen as the interconnection between two subsystems:

$$\Sigma_1 \begin{cases} \dot{X}_1 = A_1(X_2, y)X_1 + g_1(u, y, X_2, X_1) + \Pi T_l \\ y_1 = C_1 X_1 \end{cases} \tag{12}$$

$$\Sigma_2 \begin{cases} \dot{X}_2 = A_2(X_1)X_2 + g_2(u, y, X_1, X_2) \\ y_2 = C_2 X_2 \end{cases} \tag{13}$$

where $X_1 = \begin{bmatrix} i_{s\alpha} & \Omega & R_s \end{bmatrix}^T$ and $X_2 = \begin{bmatrix} i_{s\beta} & \phi_{r\alpha} & \phi_{r\beta} \end{bmatrix}^T$ are respectively the state vectors of (12) and (13), and:

$$A_1(X_2, y) = \begin{bmatrix} 0 & a_3 p\phi_{r\beta} & -a_3 i_{s\alpha} \\ -p\phi_{r\beta}/J & -f/J & 0 \\ 0 & 0 & 0 \end{bmatrix} \tag{14a}$$

$$A_2(X_1) = \begin{bmatrix} -a_3 a_1 & -a_3 p\Omega & \delta \\ 0 & -\delta L_{esq} & -p\Omega \\ 0 & p\Omega & -\delta L_{esq} \end{bmatrix} \tag{14b}$$

$$g_1(u, y, X_2, X_1) = \begin{bmatrix} -a_3 a_1 i_{s\alpha} + \delta\phi_{r\alpha} + a_3 u_{s\alpha} \\ \frac{p}{J}\phi_{r\alpha} i_{s\beta} \\ 0 \end{bmatrix} \tag{14c}$$

$$g_2(u, y, X_2, X_1) = \begin{bmatrix} -a_3 R_s i_{s\beta} + a_3 u_{s\beta} \\ a_1 i_{s\alpha} \\ a_1 i_{s\beta} \end{bmatrix} \tag{14d}$$

$$C_1 = C_2 = \begin{bmatrix} 1 & 0 & 0 \end{bmatrix} \tag{14e}$$

$u = [u_{s\alpha} \quad u_{s\beta}]^T$ and $y = [i_{s\alpha} \quad i_{s\beta}]^T$ are respectively the input and output of the physical induction machine.

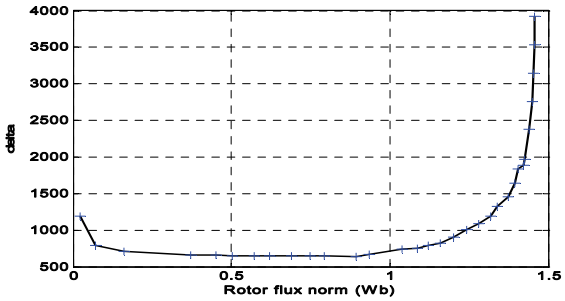

Fig.2. Characteristic ($\delta(\Omega H^{-2})$, Φ_r (Wb)). Directly computed points (++) and polynomial interpolation (solid).

A. Observer design

The design strategy consists in synthesizing separately an observer for each one of the subsystems (12) and (13). When focusing on one subsystem, the state of the other is supposed to be available (Fig 3). The global observer (that applies to the whole sensorless induction machine) is simply obtained by combining the separately obtained observers. The input persistency property (that is strongly linked to observability properties of the involved subsystems) is invoked to show that the interconnection between both observers works well. It is formally defined by the following assumptions:

A1. The pair (u, X_2) (resp. (u, X_1)) is a bounded and persistently exciting input for Σ_1 (resp. Σ_2) in the sense of [1].

A2. The rotor speed never vanishes (to preserve subsystems observability).

These assumptions are completed by the following standard signal boundedness assumption which is coherent with the open-loop control context, presently considered:

A3. The induction machine remains in the physical operation domain, denoted $\wp$, defined as follows:

$$\wp = \{X \in IR^6 \ / \ |\phi_{r\alpha}| \le \Phi^{\max}, |\phi_{r\beta}| \le \Phi^{\max}, |i_{s\alpha}| \le I^{\max}, |i_{s\beta}| \le I^{\max}, |\Omega| \le \Omega^{\max}, |T_L| \le T_L{}^{\max} \}$$

where $X = \begin{bmatrix} i_{s\alpha} & \Omega & T_L & i_{s\beta} & \phi_{r\alpha} & \phi_{r\beta} \end{bmatrix}^T$ is the whole state vector and ($\Phi^{\max}$, $I^{\max}$, Ω^{MAX}, $T_L{}^{\max}$) are the maximal values that the real variables (i.e. fluxes, currents, speed and load torque) can physically take.

Remark 1. Using A3, it is easily checked by simple inspection of (1)-(9) that:

i) $A_1(.)$ is globally Lipschitz w.r.t. X_2,

ii) $A_2(.)$ is globally Lipschitz w.r.t. X_1,

iii) $g_1(.)$ is globally Lipschitz w.r.t. X_2 and X_1.

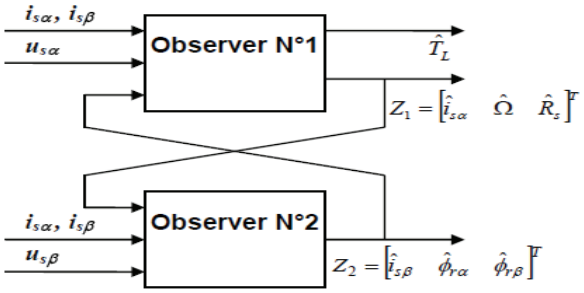

Fig.3. Interconnected observer structure

Based on the above Lipschitzian properties, the following interconnected observers are obtained applying the extended Kalman filter approach to both subsystems (11) and (12) ([12]):

$$\begin{cases} \dot{Z}_1 = A_1(Z_2,y)Z_1 + g_1(u,y,Z_2,Z_1) + \Pi\hat{T}_l \\ \quad + (\lambda\Lambda S_3^{-1}\Lambda^T + \Gamma S_1^{-1})C_1^T(y_1 - \hat{y}_1) + KC_2^T(y_2 - \hat{y}_2) \\ \dot{\hat{T}}_l = \lambda S_3^{-1}\Lambda^T C_1^T(y_1 - \hat{y}_1) + B_1(Z_2)(y_2 - \hat{y}_2) + B_2(Z_2)(y_1 - \hat{y}_1) \\ \dot{S}_1 = -\theta_1 S_1 - A_1^T(Z_2,y)S_1 - S_1 A_1(Z_2,y) + C_1^T C_1 \\ \dot{S}_3 = -\theta_3 S_3 + \Lambda^T C_1^T C_1 \Lambda \\ \dot{\Lambda} = (A_1(Z_2,y) - \Gamma S_1^{-1} C_1^T C_1)\Lambda + \Pi \\ \hat{y}_1 = C_1 Z_1 \end{cases} \tag{15}$$

$$\begin{cases} \dot{Z}_2 = A_2(Z_1)Z_2 + g_2(u,y,Z_1,Z_2) + S_2^{-1}C_2^T(y_2 - \hat{y}_2) \\ \dot{S}_2 = -\theta_2 S_2 - A_2^T(Z_1)S_2 - S_2 A_2(Z_1) + C_2^T C_2 \\ \hat{y}_2 = C_2 Z_2 \end{cases} \tag{16}$$

where $Z_1 = [\hat{i}_{s\alpha} \quad \hat{\Omega} \quad \hat{R}_s]^T$ and $Z_2 = [\hat{i}_{s\beta} \quad \hat{\phi}_{r\alpha} \quad \hat{\phi}_{r\beta}]^T$ are the estimates of the state vectors X_1 and X_2, respectively; (θ_1, θ_2, θ_3) are positive real constants and (S_1, S_2) are symmetric positive definite matrices [1]. $S_3(0) > 0$, $B_1(Z_2) = k\frac{p}{J}\hat{\phi}_{r\alpha}$, $B_2(Z_2) = -k\frac{p}{J}\hat{\phi}_{r\beta}$. Note that the estimate $\hat{\delta}$ of δ is simply obtained by $\hat{\delta} = \mathrm{T}(\hat{\Phi}_r)$ with $\hat{\Phi}_r = \sqrt{(\hat{\phi}_{r\alpha}^2 + \hat{\phi}_{r\beta}^2)}$.

$$K = \begin{bmatrix} -k_{c1} & 0 & 0 \\ -k_{c2} & 0 & 0 \\ 0 & 0 & 0 \end{bmatrix}, \ \Gamma = \begin{bmatrix} 1 & 0 & 0 \\ 0 & 1 & 0 \\ 0 & 0 & \alpha \end{bmatrix} \tag{17}$$

with k, k_{c1}, k_{c2}, α, and ϖ as positive constants.

Remark 2. The term $B_1(Z_2)(y_2 - \hat{y}_2) + B_2(Z_2)(y_1 - \hat{y}_1)$ in (15) is explicitly rewritten as follows:

$$\begin{aligned} & B_1(Z_2)(y_2 - \hat{y}_2) + B_2(Z_2)(y_1 - \hat{y}_1) \\ & \quad = k\left[\frac{p}{J}(\hat{\phi}_{r\alpha} i_{s\beta} - \hat{\phi}_{r\beta} i_{s\alpha}) - \frac{p}{J}(\hat{\phi}_{r\alpha}\hat{i}_{s\beta} - \hat{\phi}_{r\beta}\hat{i}_{s\alpha})\right] \\ & \quad = k(T_e - \hat{T}_e) \end{aligned} \tag{18}$$

with T_e and $\hat{T}_e$ are respectively, the measured and estimated electromagnetic torques.

B. *Observer stability analysis*

The analysis is performed considering uncertainties of the induction machine. Specifically, the true model is obtained by augmenting the nominal model (12)-(13) as follows:

$$\Sigma_1 \begin{cases} \dot{X}_1 = A_1(X_2,y)X_1 + g_1(u,y,X_2,X_1) + \Pi T_l \\ \quad + \Delta A_1(X_2,y)X_1 + \Delta g_1(u,y,X_2,X_1) \\ y_1 = C_1 X_1 \end{cases} \tag{19}$$

$$\Sigma_2 \begin{cases} \dot{X}_2 = A_2(X_1)X_2 + g_2(u,y,X_1,X_2) \\ \quad + \Delta A_2(X_1)X_2 + \Delta g_2(u,y,X_1,X_2) \\ y_2 = C_2 X_2 \end{cases} \tag{20}$$

with $\Delta A_1(.)$, $\Delta A_2(.)$, $\Delta g_1(.)$, and $\Delta g_2(.)$ as uncertain terms of $A_1(.)$, $A_2(.)$, $g_1(.)$, $g_2(.)$, respectively.

Using assumption A3, it follows, from (21a-d) and (14a-d) that there exist positive constants $\rho_i > 0$ ($i = 1,\ldots,4$):

$$\|\Delta A_1(X_2,y)\| \le \rho_1 \tag{22}$$

$$\|\Delta A_2(X_1)\| \le \rho_2 \tag{23}$$

$$\|\Delta g_1(u,y,X_1,X_2)\| \le \rho_3 \tag{24}$$

$$\|\Delta g_2(u,y,X_1,X_2)\| \le \rho_4 \tag{25}$$

To analyze the observer convergence, introduce the following estimation errors:

$$e_1' = X_1 - Z_1; \ e_2 = X_2 - Z_2 \ , \ e_3 = T_L - \hat{T}_L \tag{26}$$

Then, it follows from (12)-(13) and (15)-(16) that these errors undergo the following equations:

$$\begin{aligned} \dot{e}_1' = & \left[A_1(Z_2,y) - \lambda\Lambda S_3^{-1}\Lambda^T C_1^T C_1 - \Gamma S_1^{-1} C_1^T C_1\right] e_1' \\ & + \Pi \, e_3 - KC_2^T C_2 e_2 \\ & + \left[A_1(X_2,y) + \Delta A_1(X_2,y) - A_1(Z_2,y)\right] X_1 \\ & + g_1(u,y,X_1,X_2) + \Delta g_1(u,y,X_1,X_2) \\ & - g_1(u,y,Z_1,Z_2) \end{aligned} \tag{27}$$

$$\begin{aligned} \dot{e}_2 = & \left[A_2(Z_1) - S_2^{-1}C_2^T C_2\right] e_2 \\ & + \left[A_2(X_1,y) + \Delta A_2(X_1,y) - A_2(Z_1,y)\right] X_2 \\ & + g_2(u,y,X_1,X_2) + \Delta g_2(u,y,X_1,X_2) \\ & - g_2(u,y,Z_1,Z_2) \end{aligned} \tag{28}$$

$$\dot{e}_3 = -\lambda S_3^{-1}\Lambda^T C_1^T C_1 e_1' - B_1(Z_2)C_2 e_2 - B_2(Z_2)C_1 e_1' \tag{29}$$

Introducing the transformation

$$e_1 = e_1' - \Lambda e_3 \tag{30a}$$

one readily gets:

$$\dot{e}_1 = \dot{e}_1' - \dot{\Lambda} e_3 - \Lambda \dot{e}_3 \tag{30b}$$

Using (12a-c) and (7), it follows from (13) that:

$$\begin{aligned} \dot{e}_1 = & \left[A_1(Z_2,y) - \Gamma S_1^{-1} C_1^T C_1 + B_{21}\right] e_1 + (B_{12} - K') e_2 \\ & + g_1(u,y,X_1,X_2) + \Delta g_1(u,y,X_1,X_2) - g_1(u,y,Z_1,Z_2) \\ & \left[A_1(X_2,y) + \Delta A_1(X_2,y) - A_1(Z_2,y)\right] X_1 + B_{22} e_3 \end{aligned} \tag{31}$$

$$\begin{aligned} \dot{e}_2 = & \left[A_2(Z_1) - S_2^{-1}C_2^T C_2\right] e_2 + \left[A_2(X_1) + \Delta A_2(X_1) - A_2(Z_1)\right] X_2 \\ & + g_2(u,y,X_1,X_2) + \Delta g_2(u,y,X_1,X_2) - g_2(u,y,Z_1,Z_2) \end{aligned} \tag{32}$$

$$\begin{aligned} \dot{e}_3 = & -\left[\lambda S_3^{-1}\Lambda^T C_1^T C_1 \Lambda + B_2'\right] e_3 \\ & - \left[\lambda S_3^{-1}\Lambda^T C_1^T C_1 + B_2''\right] e_1 - B_1' e_2 \end{aligned} \tag{33}$$

with $B_{21} = \Lambda B_2(Z_2)C_1$, $B_{12} = \Lambda B_1(Z_2)C_2$,

$B_{22} = \Lambda B_2(Z_2) C_1 \Lambda$, $B_2'' = B_2(Z_2) C_1$, $B_1' = B_1(Z_2) C_2$ and $K' = K C_2^T C_2$.

Letting $\|e_1\|_{S_1}^2 \overset{def}{=} e_1^T S_1 e_1$; $\|e_2\|_{S_2}^2 \overset{def}{=} e_2^T S_2 e_2$, and $\|e_3\|_{S_3}^2 \overset{def}{=} e_3^T S_3 e_3$ one has:

$$\lambda_{\min}(S_1)\|e_1\|^2 \le \|e_1\|_{S_1}^2 \le \lambda_{\max}(S_1)\|e_1\|^2 \quad (34)$$

$$\lambda_{\min}(S_2)\|e_2\|^2 \le \|e_2\|_{S_2}^2 \le \lambda_{\max}(S_2)\|e_2\|^2 \quad (35)$$

$$\lambda_{\min}(S_3)\|e_3\|^2 \le \|e_3\|_{S_3}^2 \le \lambda_{\max}(S_3)\|e_3\|^2 \quad (36)$$

where $\lambda_{\min}(S_1)$, $\lambda_{\max}(S_1)$, $\lambda_{\min}(S_2)$, $\lambda_{\max}(S_2)$ and $\lambda_{\min}(S_3)$, $\lambda_{\max}(S_3)$ are the minimal, and maximal respectively eigenvalues of S_1 , S_2 and S_3 respectively.

Theorem 1. *Consider the system (19)-(20) subject to assumptions A1-A3 and the state observer (15)-(16). Let the observer gains θ_1, θ_2 and θ_3 be chosen so that the following three inequalities hold:*

$$\gamma_1 \overset{def}{=} \theta_1 - 2k_{12} - 2k_1 k_{16} - \tilde{\mu}\upsilon_1 - \tilde{\mu}_8 \upsilon_2 \quad (37)$$

$$\gamma_2 \overset{def}{=} \theta_2 - 2k_5 k_{17} - \frac{\tilde{\mu}}{\upsilon_2} - \tilde{\mu}_9 \upsilon_3 \quad (38)$$

$$\gamma_3 \overset{def}{=} \theta_3 + 2k_{12} - \frac{\tilde{\mu}_8}{\upsilon_2} - \frac{\tilde{\mu}_9}{\upsilon_2} \quad (39)$$

with

$\mu_1 = k_1 k_2 k_3$; $\mu_2 = k_1 k_4$; $\mu_3 = k_5 k_6 k_7$; $\mu_4 = k_5 k_8$;
$\mu_5 = k_1(k_{11} - k_{14})$; $\mu_6 = 2(k_1 k_3 \rho_1 + k_1 \rho_3)$;
$\mu_7 = 2(k_5 k_7 \rho_2 + k_5 \rho_4)$, $\mu_8 = k_1 k_{13} - (\lambda k_{19} + k_{18})$;
$\mu_9 = -k_{15} k_9 + k_5 k_{20} k_7)$;

$\tilde{\mu} = \sum_{j=1}^{5} \tilde{\mu}_j$ $\tilde{\mu}_j = \dfrac{\mu_j}{\sqrt{\lambda_{\min}(S_1)}\sqrt{\lambda_{\min}(S_2)}}$ and $j = 1,...,5$,

$\tilde{\mu}_8 = \dfrac{\mu_8}{\sqrt{\lambda_{\min}(S_1)}\sqrt{\lambda_{\min}(S_3)}}$, $\tilde{\mu}_9 = \dfrac{\mu_9}{\sqrt{\lambda_{\min}(S_2)}\sqrt{\lambda_{\min}(S_3)}}$,

$\tilde{\mu}_6 = \dfrac{\mu_6}{\sqrt{\lambda_{\min}(S_1)}}$, $\tilde{\mu}_7 = \dfrac{\mu_7}{\sqrt{\lambda_{\min}(S_2)}}$.

where, $\upsilon_i (i = 1,2,3) \in]0,1[$ are arbitrary, and k_1 to k_{20} are positive real constants defined in the proof. Then, one has the following properties:

1) *The observation error vector (e_1, e_2, e_3) is globally asymptotically convergent to a neighbourhood of the origin that can be made arbitrarily small by letting the θ_i 's be sufficiently large.*
2) *When the machine parameters are perfectly known (which means that the ρ_i 's are all null), the error vector (e_1, e_2, e_3) is globally exponentially vanishing* □

Proof. Consider the Lyapunov function candidate:

$$V = V_1 + V_2 + V_3 , \quad (40)$$

with:

$$V_1 = e_1^T S_1 e_1 , \; V_2 = e_2^T S_2 e_2 , \; V_3 = e_3^T S_3 e_3 \quad (41)$$

Using (15-16), (27-30) and assumption A3, one gets from (40):

$$\begin{aligned}
\dot{V} = {} & e_1^T \left\{ -\theta_1 S_1 - 2 S_1 \Gamma S_1^{-1} C_1^T C_1 - C_1^T C_1 + 2 S_1 B_{21} \right\} e_1 \\
& + 2 e_1^T S_1 \left(A_1(X_2, y) - A_1(Z_2, y) + \Delta A_1(X_2, y) \right) X_1 \\
& + 2 e_1^T S_1 \{ g_1(u, y, X_1, X_2) - g_1(u, y, Z_1, Z_2) + \Delta g_1(u, y, X_1, X_2) \} \\
& + e_3^T \left\{ -\theta_3 S_3 - 2 S_3 B_2' - (2\lambda - 1) \Lambda^T C_1^T C_1 \Lambda \right\} e_3 \\
& + e_2^T \left\{ -\theta_2 S_2 - C_2^T C_2 \right\} e_2 \\
& + 2 e_2^T S_2 \left(A_2(X_1) - A_2(Z_1) + \Delta A_2(X_1) \right) X_2 \\
& + 2 e_2^T S_2 \{ g_2(u, y, X_1, X_2) - g_2(u, y, Z_1, Z_2) + \Delta g_2(u, y, X_1, X_2) \} \\
& + 2 e_1^T S_1 (B_{12} - K') e_2 + 2 e_1^T S_1 B_{22} e_3 \\
& - 2 e_3^T (B_2'' + \lambda \Lambda^T C_1^T C_1) e_1 - 2 e_3^T S_3 B_1' e_2
\end{aligned} \quad (42)$$

According to Assumption A3 and initializing the IM drives and the observer in the physical domain D, one gets

$$\begin{aligned}
& \|S_1\| \le k_1 , \quad \|S_2\| \le k_5 , \quad \|X_1\| \le k_3 , \quad \|X_2\| \le k_7 \\
& \|g_1(u, y, X_2, X_1) - g_1(u, y, Z_2, Z_1)\| \le k_4 \|e_2\| + k_{16} \|e_1\| \\
& \|A_1(X_2, y) - A_1(Z_2, y)\| \le k_2 \|e_2\| \\
& \|A_2(X_1) - A_2(Z_1)\| \le k_6 \|e_1\| + k_{20} \|e_3\| \\
& \|g_2(u, y, X_2, X_1) - g_2(u, y, Z_2, Z_1)\| \le k_8 \|e_1\| + k_{17} \|e_2\| \\
& \|B_1'\| \le k_9 , \quad \|B_2'\| \le k_{10} , \quad \|B_2''\| \le k_{18} \\
& \|B_{12}\| \le k_{11} , \quad \|B_{21}\| \le k_{12} , \quad \|B_{22}\| \le k_{13} \\
& \|K'\| \le k_{14} , \quad \|\Lambda^T C_1^T C_1\| \le k_{19} , \quad \|S_3\| \le k_{15}
\end{aligned} \quad (43)$$

Substituting (43) into (42), from Assumption3, one has

$$\begin{aligned}
\dot{V} \le {} & -(\theta_1 - 2k_{12} - 2k_1 k_{16}) e_1^T S_1 e_1 \\
& - (\theta_2 - 2k_5 k_{17}) e_2^T S_2 e_2 - (\theta_3 + 2k_{10}) e_3^T S_3 e_3 \\
& + 2(\mu_1 + \mu_2 + \mu_3 + \mu_4 + \mu_5) \|e_1\| \|e_2\| + \mu_7 \|e_2\| \\
& + 2\mu_9 \|e_2\| \|e_3\| + 2\mu_8 \|e_1\| \|e_3\| + \mu_6 \|e_1\|
\end{aligned} \quad (44)$$

then

$$\begin{aligned}
\dot{V} \le {} & -(\theta_1 - 2k_{12} - 2k_1 k_{16}) V_1 \\
& - (\theta_2 - 2k_5 k_{17}) V_2 - (\theta_3 + 2k_{10}) V_3 \\
& + 2\tilde{\mu}\sqrt{V_1}\sqrt{V_2} + \tilde{\mu}_7 \sqrt{V_2} \\
& + 2\tilde{\mu}_9 \sqrt{V_2}\sqrt{V_3} + 2\tilde{\mu}_8 \sqrt{V_1}\sqrt{V_3} + \tilde{\mu}_6 \sqrt{V_1}
\end{aligned} \quad (45)$$

Using the following inequalities:

$$\sqrt{V_1}\sqrt{V_2} \le \frac{\upsilon_1}{2} V_1 + \frac{1}{2\upsilon_1} V_2 \quad (46a)$$

$$\sqrt{V_1}\sqrt{V_3} \le \frac{\upsilon_2}{2} V_1 + \frac{1}{2\upsilon_2} V_3 \quad (46b)$$

$$\sqrt{V_2}\sqrt{V_3} \le \frac{\upsilon_3}{2} V_2 + \frac{1}{2\upsilon_3} V_3 \quad (46c)$$

where $\upsilon_i (i = 1,2,3) \in]0,1[$ are arbitrary, and substituting (46) into (45), one gets

$$\begin{aligned}
\dot{V} \le {} & -(\theta_1 - 2k_{12} - 2k_1 k_{16} - \tilde{\mu}\upsilon_1 - \tilde{\mu}_8 \upsilon_2) V_1 \\
& - \left(\theta_2 - 2k_5 k_{17} - \frac{\tilde{\mu}}{\upsilon_2} - \tilde{\mu}_9 \upsilon_3 \right) V_2 \\
& - \left(\theta_3 + 2k_{12} - \frac{\tilde{\mu}_8}{\upsilon_2} - \frac{\tilde{\mu}_9}{\upsilon_3} \right) V_3 + \tilde{\mu}_6 \sqrt{V_1} + \tilde{\mu}_7 \sqrt{V_2}
\end{aligned} \quad (47)$$

which gives

$$\dot{V} \le -\gamma\left(V_1 + V_2 + V_2\right) + \mu(\sqrt{V_1} + \sqrt{V_2}) \le -\gamma V + \mu\vartheta\sqrt{V} \quad (48)$$

with $\gamma = \min(\gamma_1, \gamma_2, \gamma_3)$ and $\mu = \max(\mu_6, \mu_7)$ and $\vartheta > 0$ so that $\vartheta\sqrt{V_1 + V_2 + V_3} > \sqrt{V_1} + \sqrt{V_2}$.

In the rest of the present analysis, we will prove the existence of an invariance region for the function V. Let us introduce the following functions:

$$Q_1(V) = \gamma V \quad \text{and} \quad Q_2(V) = \mu\vartheta\sqrt{V} \quad (49)$$

Figure 4 shows that the curves $Q_1(V)$ and $Q_2(V)$ intersect at point A with abscissa:

$$V_A = \left(\mu\vartheta/\gamma\right)^2 \quad (50)$$

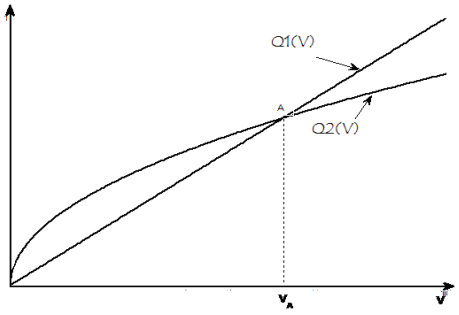

Fig. 4: Graphical plots of the functions $Q_1(V)$ and $Q_2(V)$

Then, it follows from (48) that $\dot{V}$ is negative definite whenever the initial conditions are such that $0 \le V(0) < V_A$. The error system (26)-(30) for (e_1, e_2, e_3) is asymptotically stable and the set $0 \le \|e_1\|_{S_1}^2 + \|e_2\|_{S_2}^2 + \|e_3\|_{S_3}^2 < V_A$ is a region of attraction. This establishes part 1 of the theorem.

To prove part 2, suppose that all machine parameters are perfectly known. Then, it follows from (22)-(25) that $\sigma_1 = \sigma_2 = \sigma_3 = \sigma_4 = 0$ which (by definition of μ_6 and μ_7) implies $\mu_6 = \mu_7 = 0$. In view of (36b), one gets $\mu = 0$. Then, (48) becomes:

$$\dot{V} \le -\gamma V \quad (51)$$

This implies clearly implies that the (e_1, e_2)-system is globally exponentially stable and the proof of the theorem is completed. ■

IV. SIMULATION RESULTS

The interconnected observer (15)-(16) is now evaluated, through simulation, using a 7.5 kW induction machine whose characteristics are summarized in Table 1. The observer performances will be illustrated, designing an experimental protocol that makes the machine works in open-loop. The applied load torque, input stator voltage ($V_s = 120V$) and the stator current frequency are profiled so that the machine is enforced to operate successively in the linear and nonlinear zones of its magnetic characteristic. Specifically, the machine operates in the linear part ($\Phi_r \le 1\,Wb$) over the interval $[0, 4.5\,s]$ and operates in the saturation region ($\Phi_r \ge 1.1\,Wb$) over $[4.5\,s, 10\,s]$ (see figs 6 and 8). The parameters of the design observer are given the following values which proved to be appropriate: $\theta_1 = 100$, $\theta_2 = 200$, $\theta_3 = 200$, $\lambda = 1$, $\alpha = 1$, $k_{c1} = 1$, $k_{c2} = 0.1$, $k = 0.1$, In all experiments, the initial conditions of the observed variables are different from the true values of the variables (Figs 5 and 8). Figure 5 shows the estimated stator resistance and applied load torque. Figure 6 compares the estimated and the measured rotor flux norm. It is seen (especially from the lower curve) that the estimation error rapidly vanishes. Similar results are obtained for stator current estimation (fig 7) and rotor speed estimation (figs 8). Figures 9 and 10 show the simulation results with stator resistance variation (+40%).

In summary, it is observed by figures 6 to 10 that the interconnected observer (15)-(16) performs well both in the linear region of the magnetic characteristic (time-interval $[0, 4.5\,s]$) and in the nonlinear region (time-interval $[4.5\,s, 10\,s]$). The state estimates converge to their true values after a transient period that lasts less than 0.3s.

V. CONCLUSION

The problem of estimating the magnetic and mechanical variables of an AC machine is considered within an operational context characterized by wide range flux variations and machine parameter uncertainty. It is dealt with, using an interconnected observer, designed via the high-gain technique, based on a model involving a nonlinear magnetic characteristic. The observer is formally shown to be exponentially convergent. This theoretical result is confirmed by simulation using the numerical parameter values of an induction motor of 7.5kW.

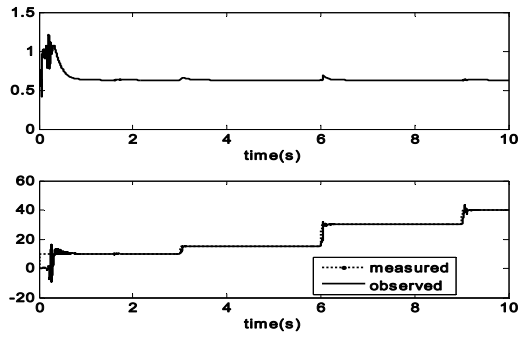

Fig. 5. Observed stator resistance in Ohm (upper fig.) and applied load torque (measured and observed) in Nm (lower fig.).

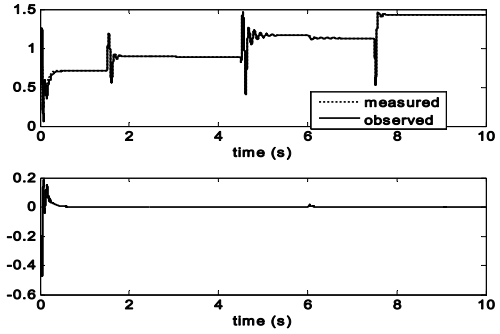

Fig 6: Rotor flux norm (Wb) estimation. Measured and observed flux norm (upper fig.), estimation error (lower fig.).

TABLE I
MOTOR CHARACTERISTICS

Nominal power	P_N	7.5	KW
Nominal voltage	U_{sn}	380	V
Nominal flux	Φ_{rn}	1	Wb
stator resistance	R_s	0.63	Ω
rotor resistance	R_r	0.4	Ω
Inertia moment	J	0.22	Kgm^2
Friction coefficient	f	0.001	N m.s rd^{-1}
Number of pole pairs	p	2	
Leakage equivalent inductance [1]	L_{seq}	7	mH

[1] Equivalent inductance of stator and rotor leakage seen from the stator

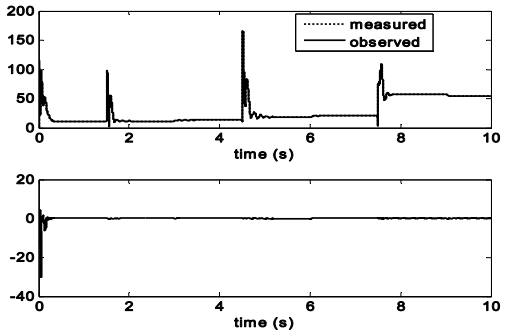

Fig 7: Stator current norm (A) estimation. Measured and estimated current norm (upper fig.), estimation error (lower fig.)

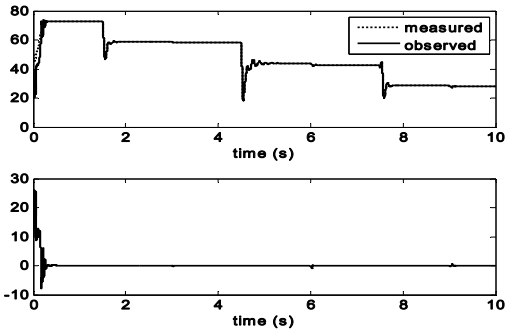

Fig 8: Mechanical speed (rd/s) estimation. Estimation error (lower fig.).

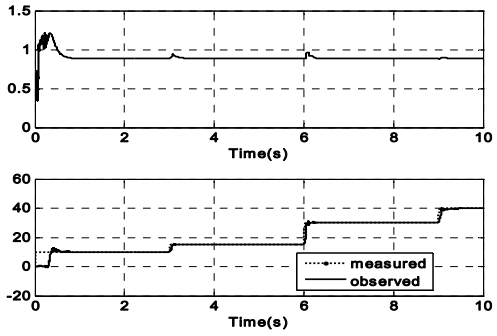

Fig. 9. Observed stator resistance and applied load torque with 40% variations in the stator resistance. Observed stator resistance in ohm (upper fig.), measured and observed load torque in Nm (lower fig.).

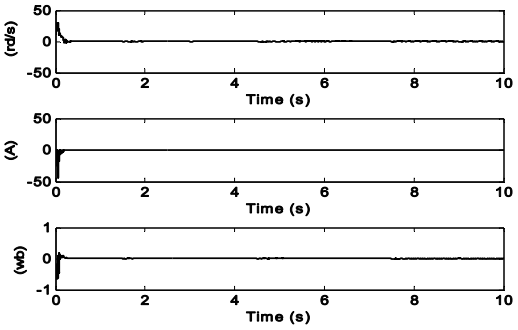

Fig. 10. All estimation errors with a +40% stator resistance variation.

REFERENCES

[1] Besançon G., G. Bornard and H. Hammouri, "Observer synthesis for a class of nonlinear control systems" , European Journal of Control, vol. 2, no. 3, pp. 176-192, 1996.

[2] De Leon-Morales, J., Alvarez-Leal J. G., Castro- Linares R., and Alvarez-Gallegos J. "Control of a flexible joint robot manipulator via a nonlinear control-observer scheme", International Journal of Control, 74(3): 290-302, 2001.

[3] Elfadili A., F. Giri, H. Ouadi, L. Dugard and A. El Magri, "Induction Machine Control in Presence of Magnetic Saturation. Speed Regulation with Optimized Flux Reference", European Control Conference, August 23-26, 2009, Budapest, Hungary.

[4] Ghanes M., J. De Leon-Morales and A. Glumineau, "Novel Controller for Induction Motor without mechanical Sensor and Experimental validation", IEEE Conference on Decision and Control (CDC), San Diego, California, USA, December 13-15, 2006.

[5] Khalil H.K., "Nonlinear systems", second edition, Prentice Hall, Upper Saddle River, 1996.

[6] Krzeminski Z. and A. Jaderko, 'Main magnetic path saturation effect in observer system of the induction motor' Proceedings of the IEEE Int. Symposium on Industrial Electronics, ISIE '93, Budapest, pp 753-758, 1993.

[7] Leonard W, "Control of Electrical Drives", Springer-Verlag, Berlin Heidelberg New York Tokyo, 1985.

[8] Lubineau D., Dion J.-M., Dugard L. and Roye D., (1999) 'Design of an advanced nonlinear controller for induction motor and experimental validation on an industrial benchmark', EPJ Applied Physics, Vol 9, pp. 967-98

[9] Ouadi H., F. Giri and L. Dugard. "Modelling saturated induction motors", IEEE Conference on Control Applications (CCA'04), Taipei, Taiwan, Vol.1, pp. 75 – 80, 2004.

[10] Ouadi H, F. Giri, J. de Leon-Morales and L. Dugard, " High gain observer design for induction motor with non linear magnetic characteristic' IFAC Word Congress, Prague, 2005.

[11] Traore D, F Plestan, A. Glumineau and J. de Leon-Morales. "Sensorless Induction motor: high order sliding mode controller and adaptive interconnected observer", IEEE Transactions on Industrial Electronics, Vol. 55, N° 11, 2008.

[12] Zhang Q, A. Xu and G. Besançon, "An efficient nonlinear adaptive observer with global convergence", 13th Symposium on System Identification (SYSID), Rotterdam 2003, IFAC / IFORS, 2003.